HHS Public Access

Author manuscript

Pediatr Res. Author manuscript; available in PMC 2017 November 01.

Published in final edited form as:

Pediatr Res. 2017 November ; 82(5): 850–854. doi:10.1038/pr.2017.155.

Somatic *PIK3CA* Mutations are Present in Multiple Tissues of Facial Infiltrating Lipomatosis

Javier A. Couto[1], **Dennis J. Konczyk**[1], **Matthew P. Vivero**[1], **Harry P.W. Kozakewich**[2], **Joseph Upton**[1], **Xi Fu**[1], **Bonnie L. Padwa**[1], **John B. Mulliken**[1], **Matthew L. Warman**[3,4,5], and **Arin K. Greene**[1]

[1]Department of Plastic & Oral Surgery, Boston Children's Hospital, Boston MA

[2]Department of Pathology, Boston Children's Hospital, Boston MA

[3]Department of Orthopaedic Surgery, Boston Children's Hospital, Boston MA

[4]Department of Genetics, Harvard Medical School, Boston MA

[5]Howard Hughes Medical Institute, Boston Children's Hospital, Boston, MA

Abstract

BACKGROUND—Facial infiltrating lipomatosis (FIL) is a congenital disorder that causes overgrowth of one side of the face. The purpose of this study was to determine if *PIK3CA* mutations are present in tissues outside of the subcutaneous adipose.

METHODS—FIL tissues from 3 patients were dissected to enrich for cells from skin, subcutaneous tissue, orbicularis oris muscle, buccal fat, zygomatic bone, and mucosal neuroma. Endothelial cells within affected tissue also were enriched using CD31-microbeads. Laser capture microdissection on formalin-fixed paraffin-embedded histologic sections was performed to collect specific cell types. DNA was extracted from each tissue and cell type, and measured for the abundance of mutant *PIK3CA* alleles using droplet digital PCR.

RESULTS—We detected mutant *PIK3CA* alleles in every tissue and cell type tested from each overgrown face; frequencies ranged from 1.5% to 53%. There were fewer mutant endothelial cells compared to non-endothelial cells, and the stromal cell compartment had the highest frequency of mutant cells in each tissue.

CONCLUSIONS—*PIK3CA* mutations are not restricted to a single tissue or cell type in FIL. Overgrowth in this condition is likely due to the mutation arising in a cell that contributes to several different facial structures during embryogenesis.

INTRODUCTION

Facial infiltrating lipomatosis (FIL) is a non-hereditary disorder characterized by hemifacial overgrowth with significant subcutaneous adipose hypertrophy. Patients have enlargement of

Corresponding Author, Arin K. Greene, MD, MMSc, Department of Plastic & Oral Surgery, Boston Children's Hospital, 300 Longwood Ave., Boston, MA 02115, Phone: 617.355.2306, Fax: 617.738.1657, arin.greene@childrens.harvard.edu.

The authors declare no conflict of interest.

one-side of the face, and also can have mucosal neuromas, hemimacroglossia, bony hypertrophy, and premature dental eruption (1, 2). We previously reported that subcutaneous adipose tissue from affected areas of patients with FIL contains somatic activating mutations in *PIK3CA* (E453K, E542K, H1047R, H1047L), a gene encoding the catalytic component of phosphatidylinositol 3 kinase (3). Thus, FIL is part of the *PIK3CA*-related overgrowth spectrum (PROS), along with other hypertrophy conditions caused by *PIK3CA* mutations (4). Although FIL typically is an isolated disease, patients with CLOVES (Congential Lipomatous Overgrowth, Vascular malformations, Epidermal nevi, Scoliosis/Skeletal/Spinal anomalies) can have FIL as a component of their syndrome (5).

Because our previous study only tested for *PIK3CA* mutations in subcutaneous fat, it is unknown whether mutant cells reside exclusively in adipose tissue or are more widely distributed. The former hypothesis would suggest facial overgrowth is primarily driven by paracrine signaling from fat cells, while the latter would determine that hypertrophy is due to the presence of mutant cells in the overgrown tissues. To address these two potential mechanisms for overgrowth, we searched for *PIK3CA* mutations in multiple different cell and tissue types that were excised from patients with FIL during a clinically-indicated procedure.

METHODS

Patient Ascertainment and Sample Collection

After approval by the Committee on Clinical Investigation at Boston Children's Hospital and acquiring written consent, tissue was collected from 3 patients with FIL who underwent subtotal resection. Participant 1 was a 3-year-old male (Figure 1a), Participant 2 was an 8-year-old female, and Participant 3 was a 15-year-old female; all subjects had isolated FIL and no other co-morbidities or features associated with another PROS condition (e.g., CLOVES syndrome) (Table 1). Samples collected from the study participants included skin and subcutaneous tissue, orbicularis oris muscle, buccal fat, zygomatic bone, and/or oral mucosal neuromas. Non-affected tissue (white blood cell DNA) was acquired from 2 of the patients. In order to more precisely define cell types within specimens, some samples were formalin-fixed and paraffin-embedded so that histologic sections could be microscopically examined and used for laser capture microdissection. Because subcutaneous adipose was known to contain the *PIK3CA* mutation and was the most abundant tissue collected, a portion was used to enrich for vascular endothelial cells for all 3 participants.

Participant 1 was a 3-year-old male who was noted to have right-sided facial overgrowth at birth. He did not have any other medical problems, family history of overgrowth, or medications. On physical examination he had enlargement of the right face, as well as mucosal neuromas, macrodontia, and hemimacroglossia (Figure 1a). These features were pathognomonic for FIL. He underwent MR imaging which confirmed the diagnosis; significant adipose hypertrophy of the subcutaneous tissue with overgrowth of all structures of one side of the face. The patient did not have any features of a syndrome associated with PROS (e.g., epidermal nevus, hand/foot anomalies, spinal malformations, brain anomalies, vascular malformations).

Participant 2 was an 8-year-old female who had overgrowth of the left side of her face at birth. She did not have any other medical problems and was not taking medications. Family history was unremarkable. Physical examination showed features consistent with FIL: hemifacial overgrowth, mucosal neuromas, macrodontia, and hemimacroglossia. CT imaging confirmed adipose hypertrophy in the subcutaneous plane and overgrowth of all structures of the left face. She did not have features of another PROS condition (e.g., epidermal nevus, hand/foot anomalies, spinal malformations, brain anomalies, vascular malformations).

Participant 3 was a 15-year-old female who was noted to have overgrowth of her left face at birth. She was otherwise healthy and there was no family history of overgrowth conditions. Physical examination was pathognomonic for FIL (hemifacial enlargement, mucosal neuromas, macrodontia, hemimacroglossia). MR imaging showed subcutaneous adipose excess and overgrowth of all facial structures of the left face. She did not exhibit any features of other PROS conditions (e.g., epidermal nevus, hand/foot anomalies, spinal malformations, brain anomalies, vascular malformations).

Laser Capture Microdissection

Five micron thick formalin-fixed, paraffin-embedded tissue sections were obtained from the grossly dissected orbicularis oris muscle, buccal fat, mucosal neuroma, skin, and bone. Laser capture microdissection was used to enrich for specific cell types within these sections. From the orbicularis oris specimen, skeletal muscle cells, stromal cells, and adipocytes were collected. From the buccal fat, stromal cells and adipocytes were obtained. Osteocytes were collected from the bone. Mucosal neuroma-derived epithelial, stromal, and neural cells were isolated. From the skin, epidermis and dermis, adipocytes, and stromal cells were collected. Because tissue sections were photographed before and after laser microdissection, hematoxylin and eosin staining was done without a coverslip; water used as a surface film during photography caused a variable amount of eosin to leach out of the sections.

Laser captured specimens were suspended in 30 μL of phosphate buffered saline, to which 30 μL of 25 mM NaOH and 0.2 mM disodium EDTA, and 30 μL of 40mM Tris-HCl were sequentially added following the HotSHOT method (6). Two microliters of these HotSHOT extracted template DNAs then were used to PCR amplify the mutated region of *PIK3CA*, using previously described primers and PCR conditions (7). PCR product was quantified using a spectrophotometer (DS-11, DeNovix).

Cell Sorting and Analysis

Subcutaneous adipose tissue was washed in PBS to remove blood cell contaminants, digested with collagenase A (2.5 mg/mL) (Roche) for 1 hour at 37°C, then filtered through a 100 μm strainer to produce a single cell suspension. Cells were placed on fibronectin-coated (1 μg/cm^2) tissue culture plates (Olympus Plastics) in endothelial growth medium-2 (EGM-2, Lonza) supplemented with 10% fetal bovine serum (FBS, Gibco, Life Technologies). After 5–7 days of expansion, cells were fractionated into 2 populations (endothelial and non-endothelial) using anti-human CD31 (endothelial cell marker) magnetic beads (DynaBeads™, Life Technologies) (8). DNA was extracted from each cell

population using the QIAamp DNA Mini kit following the manufacturer's instructions (Qiagen).

Droplet Digital PCR (ddPCR)-Based Mutational Analysis

PCR primers, fluorescent probes, and methods for detecting wild-type and mutant *PIK3CA* alleles have been previously described (7). For genomic DNA that was extracted from tissue or cells, we used 30 nanograms of template DNA, corresponding to ~ 4000 cells, in each ddPCR reaction. For PCR amplimers that were produced using laser capture microdissected DNA as template, we used 0.3 femtograms of DNA, corresponding to ~ 3000 DNA molecules, in each ddPCR reaction. ddPCR was performed using a QX200 Droplet Generator, QX200 Droplet Reader, and QuantaSoft software (Bio-Rad).

RESULTS

Using ddPCR, we detected either a p.H1047R or p.H1047L missense mutant *PIK3CA* allele in every tissue- and cell-type examined from each overgrown face; a mutation was not present in unaffected tissue (white blood cell DNA) (Table 2, Figure 1). To exclude the possibility that mutant alleles in non-adipose tissues were derived from microscopic adipocyte infiltration, we examined stained histologic sections of the zygomatic bone, skin, orbicularis oris muscle, and mucosal neuroma specimens from which we extracted DNA for ddPCR. We observed only sparsely distributed adipocytes in the orbicularis oris muscle specimen. Therefore, we performed ddPCR on DNA that was recovered from the muscle, adipocyte, and stromal cell components of this specimen by laser capture microdissection (Figure 2). In the orbicularis oris specimen, the myocyte-enriched component contained 24% mutant alleles, whereas the adipocyte and stromal components contained 25% and 41% mutant alleles, respectively (Table 3). Results consistent with involvement of multiple cell types also were obtained when the buccal fat, mucosal neuroma, and skin were studied (Table 3). The stromal cell compartment contained the highest frequency of mutant cells in each section.

Because it is challenging to laser capture vascular versus non-vascular cells in order to determine whether endothelial cells were enriched for the *PIK3CA* mutation, we used an affinity bead-based method to enrich for $CD31^+$ vascular endothelial cells in each participant's subcutaneous tissue specimen. In contrast to the non-endothelial cell compartment, which had high levels of mutant cells, the endothelial cell compartment had low levels (Table 2).

DISCUSSION

Surgical resection is the only therapeutic option to treat FIL. In order to develop pharmacological interventions, previously we searched for the underlying cause of FIL and found that affected tissue contained somatic gain-of-function mutations in *PIK3CA* (E453K, E542K, H1047R, H1047L) (3). These same somatic mosaic mutations have been identified in cancers, vascular malformations, and other disorders with overgrowth (4, 7, 9). In the present study, we sought to determine if overgrowth in patients with FIL was caused by a somatic mutation in one tissue type (subcutaneous adipose) that exerts paracrine effects on

neighboring structures (10)or by the presence of mutant cells in each of a patient's overgrown tissues (11).

We found that all tissues on the side of the face affected with FIL contained *PIK3CA* (H1047R, H1047L) mutations. A similar paradigm has been found in another PROS condition (CLOVES), where a patient who had an amputated limb was noted to have *PIK3CA* mutations in multiple tissues of the overgrown extremity (12). FIL exhibited the highest mutant allele frequency in the stroma, potentially because fibroblasts might have a greater mutant allele frequency compared to other cell types. Another possibility is that mutant progenitor cells reside in the stroma that can differentiate into parenchymal cells.

FIL had been hypothesized to result from a vascular abnormality because patients often have increased cutaneous vascularity exemplified as a stain or blush (1, 2). We recently found that endothelial cells from patients with a different overgrowth syndrome, capillary malformation, are enriched for *GNAQ* mutations (13). We did not find the same enrichment of *PIK3CA* mutant endothelial cells in patients with FIL. Therefore, overgrowth in patients with FIL is unlikely to be caused by an underlying vascular abnormality. Instead, our data indicate that FIL results from a mutation in a multipotent progenitor cell that contributes to mesodermal derivatives (e.g. stroma, adipose, muscle, bone) as well as to ectodermal structures (e.g., nerves) (14, 15). If we had found that only the subcutaneous adipose tissue contained *PIK3CA* mutations, we would postulate that these adipocytes have nonautonamous effects on other facial cells that cause overgrowth. A dynamic paracrine interaction between cell types might be more favorable to develop pharmacotherapy for the disease; for example, inhibitors of paracrine signaling by subcutaneous adipose might prevent secondary overgrowth of other structures. Instead, all components of the face contain mutations that likely occurred during embryogenesis suggesting that the condition is a structural anomaly. Mice that harbor conditional alleles in *Pik3ca*, which can be activating in a cell-type and tissue specific manner, likely will be useful in further elucidating the cause of FIL.

Acknowledgments

The authors thank Lois E. Smith, MD, PhD and Zhongjie Fu, PhD from the Department of Ophthalmology, Boston Children's Hospital, for letting us use their laser capture microdissection system. This work was supported by the Translational Research Program, Boston Children's Hospital (A.K.G.), and NIH grants R21-HD082606 (A.K.G.), R21-HD081004 (A.K.G), and R01-AR064231 (M.L.W.).

References

1. Slavin SA, Baker DC, McCarthy JG, Mufarrij A. Congenital Infiltrating Lipomatosis of the Face: Clinicopathologic Evaluation and Treatment. Plast Reconstr Surg. 1983; 72:158–164. [PubMed: 6192455]
2. Padwa BL, Mulliken JB. Facial Infiltrating Lipomatosis. Plast Reconstr Surg. 2001; 108:1544–1554. [PubMed: 11711926]
3. Maclellan RA, Luks VL, Vivero MP, et al. PIK3CA Activating Mutations in Facial Infiltrating Lipomatosis. Plast Reconstr Surg. 2014; 133:12e–19e. [PubMed: 25942115]
4. Keppler-Noreuil KM, Rios JJ, Parker VE, et al. PIK3CA-related overgrowth spectrum (PROS): diagnostic and testing eligibility criteria, differential diagnosis, and evaluation. Am J Med Genet A. 2015; 167A:287–95. [PubMed: 25557259]

5. Fernandez-Pineda I, Fajardo M, Chaudry G, Alomari AI. Perinatal clinical and imaging features of CLOVES syndrome. Pediatr Radiol. 2010; 40:1436–9. [PubMed: 20155260]
6. Truett GE, Heeger P, Mynatt RL, Truett AA, Walker JA, Warman ML. Preparation of PCR-Quality Mouse Genomic DNA Hot Sodium Hydroxide and Tris (HotSHOT). Biotechniques. 2000; 29:52–54. [PubMed: 10907076]
7. Luks VL, Kamitaki N, Vivero MP, et al. Lymphatic and Other Vascular Malformative/Overgrowth Disorders are Caused by Somatic Mutations in *PIK3CA*. J Pediatr. 2015; 166:1048–1054. [PubMed: 25681199]
8. Huang L, Nakayama H, Klagsbrun M, Klagsbrun M, Mulliken JB, Bischoff J. Glucose Transporter 1-Positive Endothelial Cells in Infantile Hemangioma Exhibit Features of Facultative Stem Cells. Stem Cells. 2015; 33:133–145. [PubMed: 25187207]
9. Samuels Y, Wuang Z, Bardelli A, et al. High Frequency of Mutations of the *PIK3CA* Gene in Human Cancers. Science. 2004; 304:554. [PubMed: 15016963]
10. Brown NK, Zhou Z, Zhang J, et al. Perivascular adipose tissue in vascular function and disease: a review of current research and animal models. Arterioscler Thromb Vasc Biol. 2014; 34:1621–30. [PubMed: 24833795]
11. Couto JA, Huang L, Vivero MP, et al. Endothelial Cells from Capillary Malformations are Enriched for Somatic *GNAQ* Mutations. Plast Reconstr Surg. 2016; 137:77e–82e.
12. Kurek KC, Luks VL, Ayturk UM, et al. Somatic mosaic activating mutations in PIK3CA cause CLOVES syndrome. Am J Hum Genet. 90:1108–15. 20128. [PubMed: 22658544]
13. Couto JA, Vivero MP, Upton J, et al. Facial Infiltrating Lipomatosis Contains Somatic PIK3CA Mutations in Multiple Tissues. Plast Reconstr Surg. 2015; 136(4 Suppl):72–3. [PubMed: 26397580]
14. Pansky, B. Review of Medical Embryology. New York, New York: MacMillan Publishing Co.; 1982. Germ Layer and Their Derivatives; p. 62-63.
15. Larsen, WJ. Human Embryology. New York, New York: Churchill Livingstone Inc.; 1993. The Third Week; p. 47-63.

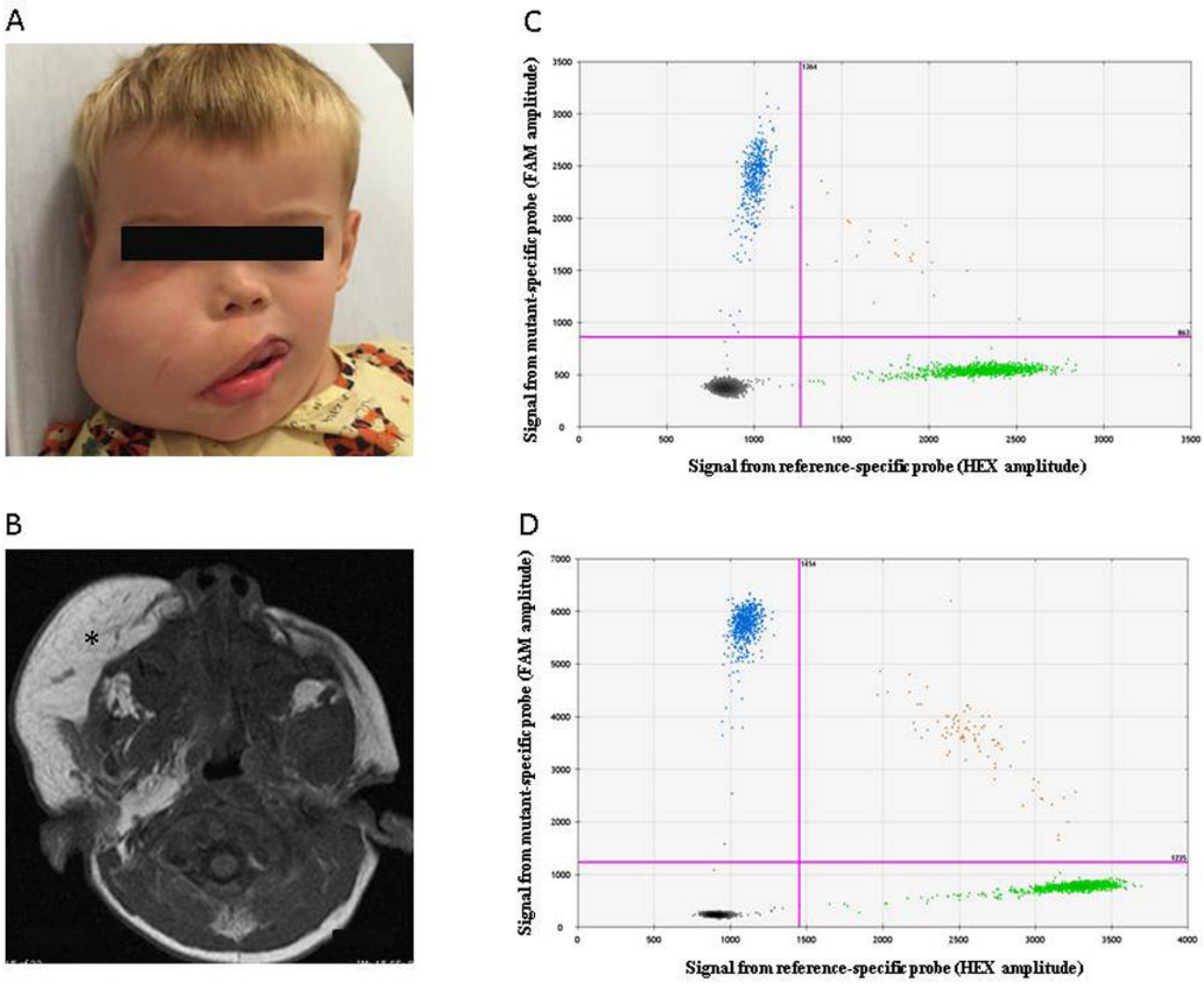

Figure 1. Clinical images and ddPCR data for Participant 1

(**a**) Three year-old male prior to a debulking procedure. (**b**) MRI shows increased subcutaneous thickening (*). (**c, d**) ddPCR assay results for DNA extracted from mucosal neuroma (c) and from zygoma (d). Droplets containing amplimers representing mutant alleles are FAM-positive (left upper quadrant). Droplets containing amplimers representing wild-type alleles are HEX-positive (right lower quadrant). Droplets with mutant and wild-type amplimers are located in the right upper quadrant. Droplets without amplimers are located in the left lower quadrant.

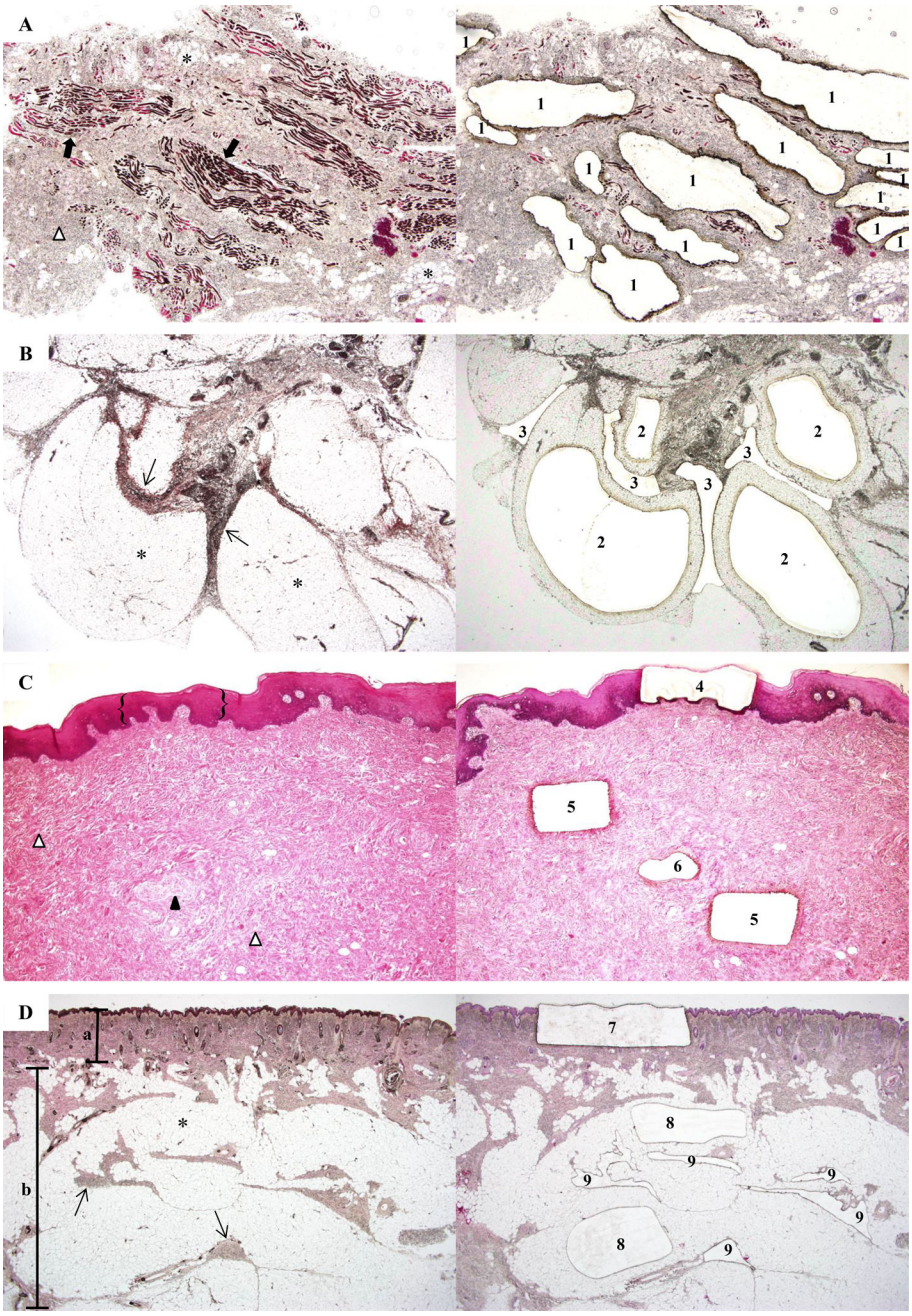

Figure 2. Laser-capture microdissection of tissue specimens from Participant 1

(**a**) (*Left*) Orbicularis oris shows striated muscle (➡), stroma (Δ), and adipocytes (*). (*Right*) Post-capture image illustrates microdissection of myocyte-enriched areas (1) (microdissection of adipocytes and stromal tissue also were performed, data not shown) (x40). (**b**) (*Left*) Buccal fat lobules composed of adipocytes (*) surrounded by fibrous septa (→). (*Right*) Tissue section after laser-capture of adipocytes (2) and septa (3) for DNA extraction (×40). (**c**) (*Left*) Mucosal neuroma comprised of the epithelium ({}), stroma (Δ), and an enlarged nerve (▲). (*Right*) Tissue section after laser-capture of epithelium (4), stroma (5), and nerve (6) (x40). (**d**) (*Left*) Skin and subcutaneous tissue section show the

epidermis and dermis (α), adipocytes (*) and fibrous septa (→) of the subcutaneous tissue (β). (*Right*) Post-capture of the epidermis and dermis (7), adipocytes (8), and stromal tissue (9) (20×). (hematoxylin & eosin staining).

Table 1

Study Cohort with Facial Infiltrating Lipomatosis

	Participant 1	Participant 2	Participant 3
PIK3CA Mutation	p.H1047R	p.H1047R	p.H1047L
Age at operation (years)	3	8	15
Sex	Male	Female	Female
Side of facial overgrowth	Right	Left	Left
Hemifacial overgrowth	+	+	+
Mucosal neuromas	+	+	+
Macrodontia	+	+	+
Hemimacroglossia	+	+	+
Epidermal nevus	−	−	−
Hand or foot anomalies	−	−	−
Spinal anomalies	−	−	−
Brain anomalies	−	−	−
Vascular malformations	−	−	−

Table 2

PIK3CA Mutant Allele Frequencies (%) in Tissues, Endothelial Cells, and Non-Endothelial Cells

Participant	Mutation	Skin	Subcutis	Muscle	Buccal Fat	Bone	Mucosal Neuroma	CD31+	CD31−
1	p.H1047R	11.4	20.1	28.2	29.0	24.6	12.8	-	49.2
2	p.H1047R	5.5	17.6	20.7	23.2	-	-	5.2	39.4
3	p.H1047L	-	16.2	5.6	-	-	-	1.5	28.0

(-) tissue not available for mutational analysis

Table 3

PIK3CA Mutant Allele Frequencies (%) in Microdissected Tissue

Specimen	Label in Figure 2	Mutant Allelic Frequency
Bone Cells		17.1
Buccal Fat		
Adipocytes	2	23.2
Stromal Cells	3	52.8
Muscle		
Skeletal Muscle Cells	1	23.7
Adipocytes	*	25.4
Stromal Cells	Δ	40.7
Oral Mucosa		
Epithelium	4	2.4
Nerves	6	32.7
Stromal Cells	5	41.3
Skin	7	17.3
Subcutis		
Adipocytes	8	25.0
Stromal Cells	9	31.9